npj | precision oncology

Article

Published in partnership with The Hormel Institute, University of Minnesota

https://doi.org/10.1038/s41698-025-00946-1

Optimized culturing yields high success rates and preserves molecular heterogeneity, enabling personalized screening for high-grade gliomas

Cassandra Posthoorn-Verheul[1], Federica Fabro[1,2,3], Ioannis Ntafoulis[1], Chelsea den Hollander[1], Iris S. C. Verploegh[1,2], Rutger Balvers[1], Trisha V. Kers[1], Jessica Hoogeveen[1], Judith van der Burg[1], Bert Eussen[4], Annelies de Klein[4], Kate J. Feller[5], Miao-Ping Chien[5], Clemens M. F. Dirven[1], Sieger Leenstra[1] & Martine L. M. Lamfers[1]

To discover new treatment options for high-grade glioma (HGG), robust in vitro models are essential, but reliably establishing patient-derived cell cultures remains challenging. We established glioma stem-like cell (GSC) cultures from 114 consecutive HGG specimens via traditional surgical resection and/or ultrasonic aspiration, using completely dissociated single cell (single cell-derived, SCD) and partially dissociated 3D-derived (3DD) tissue fragments. Higher success rates in culture establishment were obtained from ultrasonic aspirates and 3DD surgical samples. Combining these approaches yielded a 96% success rate. Copy number profiling showed overall genetic similarities between cultures and parental tissue. Single-cell sequencing revealed greater transcriptomic heterogeneity in ultrasonic aspiration-derived cultures. Our protocol enabled the screening of 20 anti-cancer agents within a clinically relevant timeframe for 16 out of 18 HGG samples. This refined protocol serves as a robust tool for establishing HGG cell cultures that retain the molecular characteristics of the tumors and support applications in precision medicine.

Glioblastoma is associated with a dismal prognosis, despite comprehensive treatment approaches. Even with extensive surgical resection and chemoradiation therapy, recurrence is inevitable, resulting in a five-year survival of only 6,9%[1]. Despite significant research efforts, the prognosis for patients afflicted with this disease has not significantly improved over the last decade. This is influenced by various contributing factors, but a major challenge is the lack of reliable in vitro models, which severely impedes research progress.

High-grade gliomas (HGG) including glioblastoma, exhibit substantial intertumoral and intratumoral heterogeneity[2–4]. For decades, glioma research relied on a limited number of cell cultures grown under serum-supplemented conditions, which failed to faithfully represent the original tumor in terms of genotype and phenotype and lacked the distinct heterogeneity characteristics of HGG[5]. Over the past two decades, there has been a shift towards utilizing patient tumor tissue in preclinical research, and culturing of patient-derived glioblastoma cells under serum-free conditions has become the gold standard. A variety of in vitro models have been developed, and these cultures are referred to as glioma stem(-like) cells (GSCs), brain-tumor initiating cells (BITCs), tumor neurospheres, or glioblastoma organoids. GSCs can be cultured in a two-dimensional (2D) manner on an extracellular matrix or in a three-dimensional (3D) format in non-adherent plates (neurospheres), whereas organoids are exclusively grown in 3D. Serum-free, patient-derived cell cultures have been reported to capture the heterogeneous cell populations present in gliomas and preserve glioma stem cells[5–7].

[1]Department of Neurosurgery, Brain Tumor Center, Erasmus Medical Center Cancer Institute, Rotterdam, The Netherlands. [2]Department of Cell Biology, Erasmus Medical Center, Rotterdam, The Netherlands. [3]Department of Developmental Biology, Erasmus Medical Center, Rotterdam, The Netherlands. [4]Department of Clinical Genetics, Erasmus Medical Center, Rotterdam, The Netherlands. [5]Department of Molecular Genetics, Erasmus Medical Center, Rotterdam, The Netherlands.
e-mail: m.lamfers@erasmusmc.nl

Despite their potential, the successful establishment of such cultures from patient samples has been challenging, with reported efficiencies ranging from 30% to 70%[6,8–13]. It is crucial to adeptly generate patient-derived cell cultures that faithfully capture the entire spectrum of molecular subtypes present in HGG. Not only for broadly applicable therapeutic strategies, but also for personalized medicine approaches. Notably, we and others have reported on the value of patient-derived HGG ex vivo assays for predicting clinical response to temozolomide, driving a surge of interest in personalized drug screening applications[14–16].

Glioma surgery poses unique challenges given the intricate location of the tumor and the necessity to safeguard the surrounding brain tissue. Traditionally, glioma cultures have been initiated using solid tumor specimens obtained through surgical resection, typically small in size. In recent years, ultrasonic aspiration (UA) devices have gained widespread use as a neurosurgical technique for tumor removal[17,18]. They enable meticulous and gentle tumor removal, both at the tumor core and at the tumor margins. Previous studies showed that UA-derived tissue fragments can be used to initiate glioblastoma cultures[19,20].

The objective of this study was to develop a tumor processing and culture protocol that would significantly enhance the establishment of patient-derived cell cultures within a clinically-relevant timeframe for personalized drug screening. We present a highly efficient method that incorporates both glioma resection material and UA-aspirate and which initiates cultures from single cells as well as from multicellular tissue fragments. The resulting cultures exhibit sustained heterogeneous RNA expression profiles across multiple passages, with greater cellular diversity observed in cultures derived through UA compared to those from tissue resection samples. The reliability and reproducibility of this approach renders it a valuable tool for studying therapy responses in glioblastoma and advancing precision medicine for HGG patients.

Results

New culture protocol allows optimal use of patient tissue for culture establishment

We have developed a tissue processing protocol for establishing cell cultures from HGG. This protocol includes both traditional surgical resection specimens as well as UA-derived samples. On average, the quantity of tumor material obtained from ultrasonic aspirates exceeds that derived from traditional resection samples (mean 3.7 ± 2.4 SD versus 1.7 ± 1.1 SD grams, respectively, $p < 0.05$) (Supplementary Fig. 1). A graphical representation of the protocol is provided in Fig. 1. Our previous protocol relied on tissue dissociation into single cells though mechanical and enzymatic dissociation, followed by filtration. Cultures initiated through this method are referred to as single-cell derived glioma stem cell (SCD-GSC) cultures in this manuscript. One of the key improvements of the new protocol is the use of multicellular three-dimensional (3D) tissue fragments that remain on the filter while straining the cell suspension after dissociation. It allows for the maximal use of tumor tissue while minimizing the damage from processing. Cultures started from these fragments are referred to as 3D-derived glioma stem cell (3DD-GSC) cultures. In the case of tumor material resected with UA, single cell-derived cultures are referred to as SCD-UA-GSC cultures, and 3D-derived cultures are referred to as 3DD-UA-GSC cultures.

Parallel use of multiple tissue processing techniques maximizes glioma culture success

In previous work based on an earlier version of the SCD-GSC culture method, we demonstrated that HGG GSC cultures can be established from single cells with an efficiency of 36%[6]. Figure 2a shows the success rate of 114 sequential HGG samples. The list includes samples from two patients who underwent multiple surgeries. Primary, secondary, recurrent and isocitrate dehydrogenase (IDH) mutant grade IV gliomas were included. Depending on the amount and type of tissue we received, we initiated as many arms of the protocol as possible. SCD-GSC cultures were established with a success rate of 69%. All the 3DD arms of the protocol significantly outperform the SCD-GSC protocol ($p < 0.05$, Fisher exact test). Moreover, 3DD-UA-GSC cultures are the most successful, with an overall success rate of 92%. If we received only a small biopsy (SB), the culture was initiated as a 3DD-SB-GSC culture. Despite the small amount of tissue, these cultures could be established at a success rate of 85%. The only HGG sample that could not be cultured with any method was a recurrent IDH mutant glioblastoma: GS.0917. Notably, the three previous attempts to establish a culture from this patient's tumor also failed, indicating that tumor-intrinsic characteristics can impede in vitro growth. Importantly, for 23 cell cultures, all four arms of the protocol were initiated in parallel (Fig. 2b). For these tumors, the combined success rate of establishing a culture was 96%.

Morphological properties, stemness, and growth characteristics

Under serum-free adherent culture conditions, established HGG cultures have characteristic morphological features when examined under a light microscope, which we previously defined as astrocytoma-like morphology[21]. These cells display an elongated shape with slender protrusions, relatively small cell bodies, well-defined edges, and noticeable space between individual cell bodies. Nevertheless, there is considerable intertumoral heterogeneity among patient-derived cell cultures, as evidenced by variations in cell size, number of protrusions, and growth patterns (Fig. 3a).

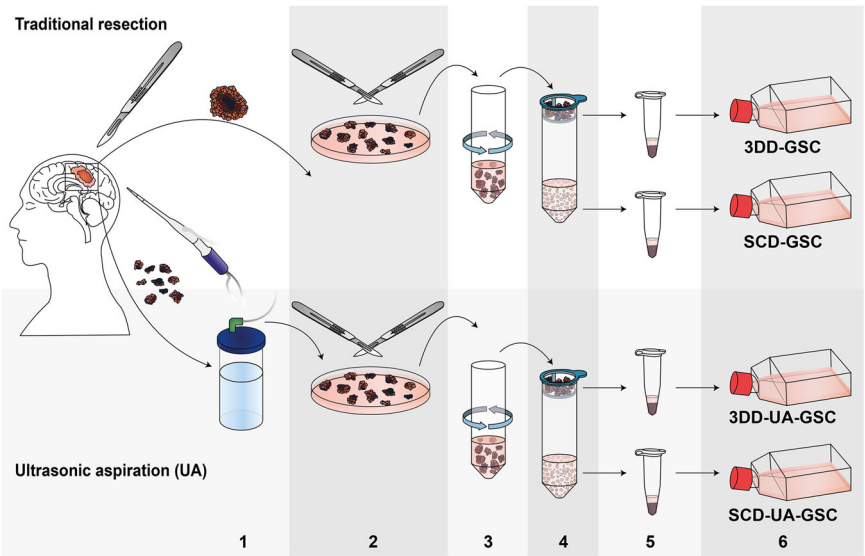

Fig. 1 | Graphical representation of the tumor processing protocol. In the operating room, tumor tissue is resected as solid pieces of tissue (step 1) or with UA (step 1). The tissue is mechanically dissociated using a scalpel (step 2) to fragments ranging in size from 0.5–3 mm. In the case of UA-samples, only the largest fragments are mechanically dissociated. Necrotic tissue, large blood vessels, and blood clots are removed. The fragments are then transferred to a 50 ml Falcon tube containing DMEM supplemented with Collagenase A and DNAse. The tubes are placed in a water bath (step 3) on a shaker for 15–30 min. Next, the suspension is passed over a 70 µm strainer (step 4). The multicellular tissue fragments that remain on top of the filter are then transferred to a separate tube. A lysis buffer is added to remove red blood cells (step 5). Finally, the pellets are washed and transferred to uncoated culture flasks in serum-free culture medium (step 6).

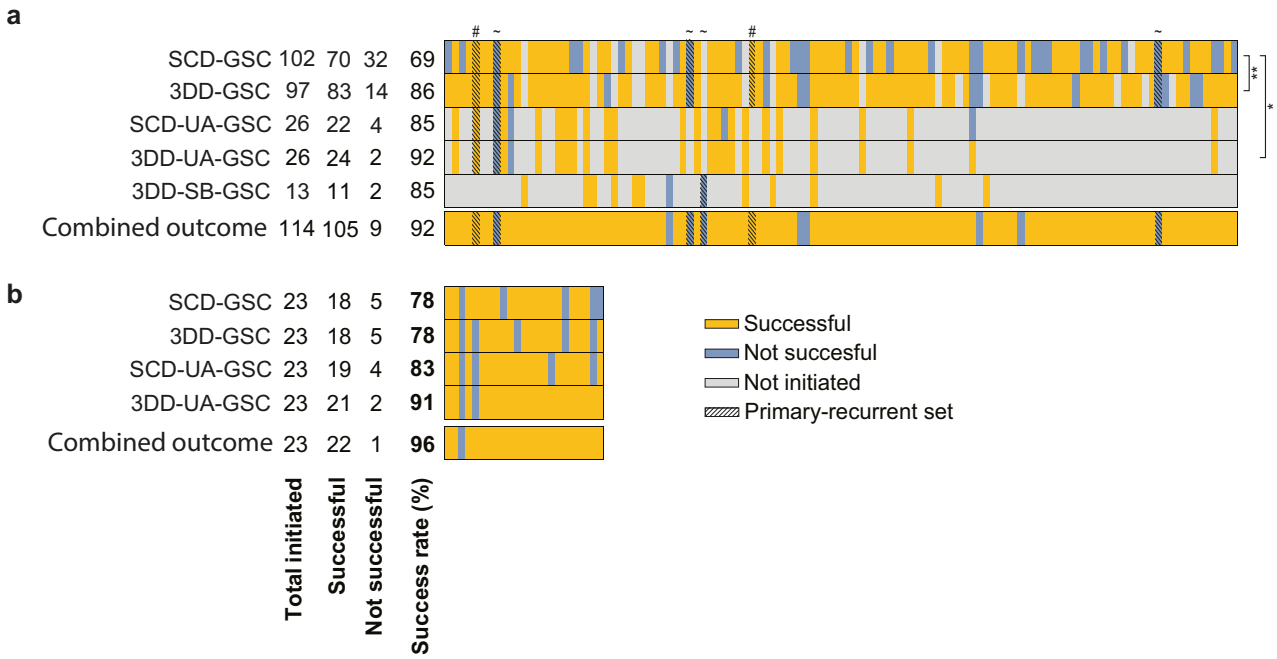

Fig. 2 | Success rate of the various arms of the culture protocol. a Graphical representation of the culture success rate per culture method. Asterisks indicate significance levels (* represents $p < 0.05$, ** represents $p < 0.01$) based on the Fisher exact contingency test. For one patient, samples from two separate surgeries were processed for culture (GS.0852 and GS.0921, designated with a hashtag). For another patient, samples from four separate surgeries were processed (GS.0917, GS.0770, GS.0866, and GS.0869, designated with a tilde). **b** Graphical representation success rate for 23 tumors for which all four parallel arms of the protocol were initiated.

For IDH mutant glioma cultures in our previous study, the astrocytoma-like cultures represented GSCs, while fibroblast-like cultures did not contain the tumor-defining mutations that were present in the parental tumors. We predicted similar findings for IDH-wildtype HGG cultures. In our hands, an estimated 5–10% of high-grade glioma cell cultures became predominantly composed of fibroblast-like cells. There appears to be no difference between the different cultural arms for this phenomenon. For instance, GS.0821 exemplifies a culture that initially exhibited mixed populations but ultimately developed into a fibroblast-like culture by passage 6 (Fig. 3b). Analysis of the B-allele frequency (BAF) plots show that the copy number events that are characteristic of this tumor did not completely vanish in culture, but the percentage of cells carrying these aberrations had diminished (Supplementary Fig. 2a, b). Such cultures should be marked as unreliable. Therefore, routine assessment of culture morphology at each passage using light microscopy should be incorporated into standard culture practices, preferably in combination with copy number variation (CNV) profiling. It is possible to pick colonies with an astrocytoma-like morphology from a culture flask and expand this to a new culture, but this will likely impact the heterogeneity of the culture.

Immunofluorescent staining of four cultures derived from a single patient (GS.0895), established through each arm of the protocol, revealed that >96% of cells in all cultures expressed the neuronal stem cell marker Sox2 (Fig. 3c). This finding aligns with expectations for cultures enriched in glioma stem cells. Additionally, glial fibrillary acidic protein (GFAP) is expressed in half the cells for the 3DD-GSC, SCD-UA-GSC, and 3DD-UA-GSC cultures, but in only 12% of the SCD-GSC cultures (Fig. 3d). Heterogeneous expression between patients of neuronal stem cell and differentiation markers was observed at the RNA level in another dataset from low-passage ($p < 10$) HGG cell culture panel from our laboratory[14].

We analyzed the growth rate of cultures derived from three separate patients, for each of the four arms of the protocol, by counting the cultures at three different passages (Fig. 3e). Multivariate linear regression modeling with Bonferroni correction showed that there was a significant effect on the growth rate between passage 4 and passage 5 (adjusted p value $p < 0.001$). Expectedly, there was a significant difference in growth rate between cultures derived from different tumors (adjusted p value $p < 0.001$). Across the samples from these three patients, the culture method did not significantly impact the growth rate, except for the 3DD-UA-GSC cultures, which demonstrated an increased growth rate compared to the other cultures (adjusted p value $p < 0.01$). Taken together, variations in cell morphological features, stem cell marker expression, and cell culture growth rate between cultures derived through different arms of the protocol appear smaller than variations observed between patient-derived cultures.

Global screening array shows overall similarity between patient tissues and derived cultures

To validate the identity of the cell cultures in this study, we utilized the Infinium Global Screening Array v2.0. We conducted a comparative analysis of copy number variation profiles between sequential tumor tissues and their corresponding cell cultures. For the 31 sequential tumor samples examined, we randomly selected one or two types of cell cultures for analysis. For three tumors, we assessed four different culture types; each obtained through a different protocol arm. Each sample was compared to its corresponding parental tissue based on the percentage of matched single nucleotide polymorphisms (SNPs), in order to confirm sample identity and to assess the level of genetic similarity between samples (Fig. 4a). All cell cultures matched with their respective parental HGG tissue samples. Furthermore, the relationship between primary IDH-wildtype glioblastoma GS.0852 and its recurrent counterpart GS.0921 is preserved in both tumor tissues and daughter cell cultures.

Integrated frequency plots show that gain of chromosome 7 and/or loss of chromosome 10 are highly common in the GBM tissues and derived cell cultures (Fig. 4b). Faithful representation of parental tissue is also demonstrated in cultures derived from all four arms of the protocol, as shown for example in GS.0902 and GS.0921. In the cultures GS.0834 and GS.0827, we observed limited chromosomal imbalances in the parental tumor tissue. However, there was an increase in copy number aberrations within the resulting cultures, likely attributed to the loss of stromal cells and the subsequent outgrowth of GSCs (Supplementary Fig. 3).

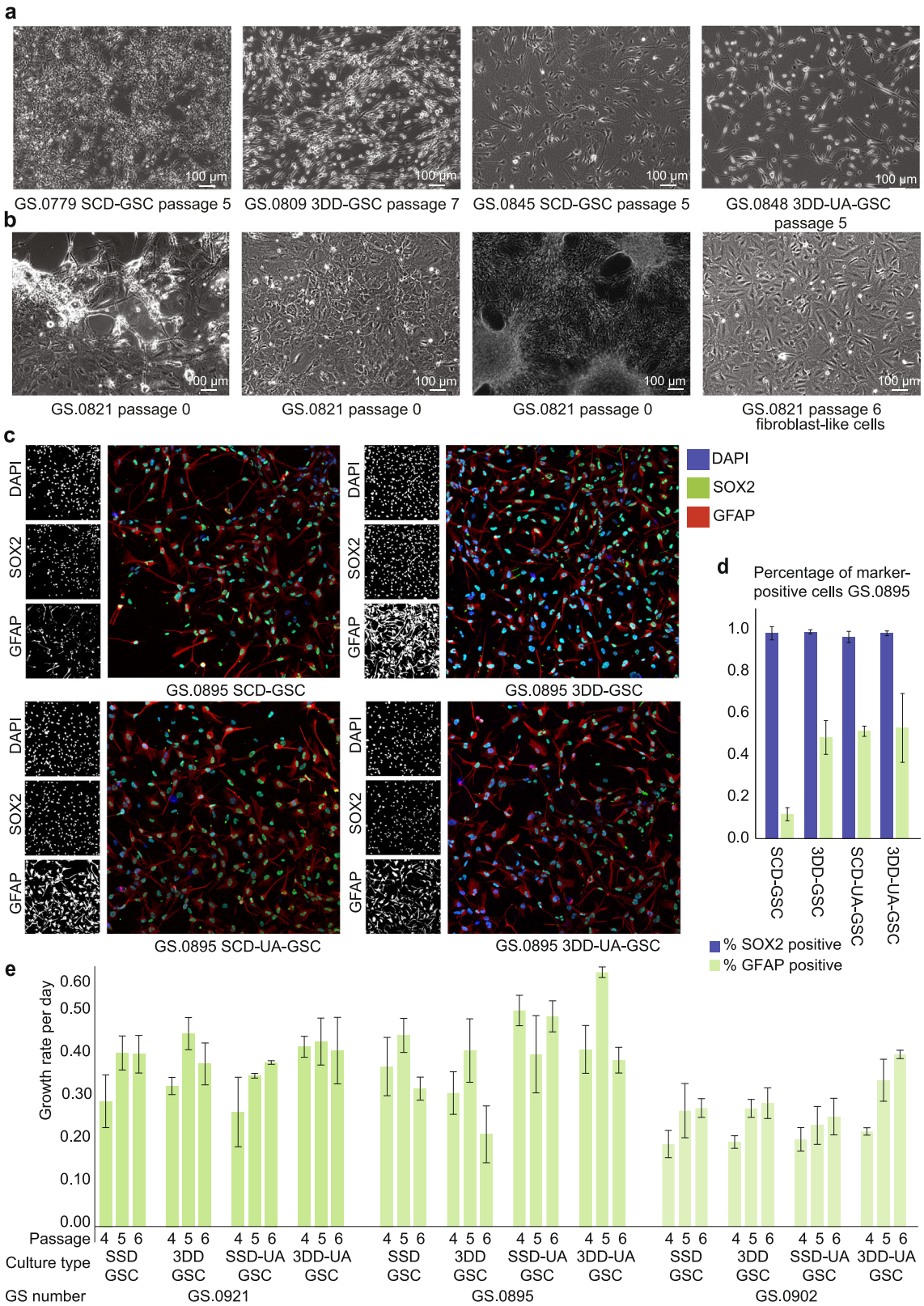

Single cell RNA sequencing confirms the retention of genetic heterogeneity and expression of HGG hallmark genes over multiple passages

HGG is known for its high degree of molecular heterogeneity, both between different tumors and within the same tumor. To assess and characterize the intra-tumoral composition of the cell cultures over time, we used single cell RNA sequencing for cultures derived from two individuals. Each patient had one culture derived from standard tissue resection (3DD-GSC) and another from UA (3DD-UA-GSC), and these cultures were sampled at four different passages (passage 1/2, 5, 11 and 16).

The analysis of the genetic profile inferred from the transcriptomic data confirmed the establishment and culturing of tumor cells. As expected, the

Fig. 3 | Adherent culture morphology can be used to identify GSC-rich cultures. **a** Brightfield images of four different representative glioma cultures (Zeiss Axio Observer D1 Inverted Phase Contrast Fluorescence Microscope, 10x magnification). All cultures show an astrocytoma-like phenotype with elongated cell shapes, slim protrusions, small cell bodies, and bright edges. Typically, unless a culture is severely overgrown, there is space between individual cell bodies. The size bar represents 100 µm. **b** Brightfield images (Zeiss Axio Observer D1 Inverted Phase Contrast Fluorescence Microscope, 10x magnification) of culture GS.0821 at passage 0 and at passage 6. At passage zero, a heterogeneous mix of two cell types can be observed: the astrocytoma-like phenotype and the fibroblast-like phenotype. **c** Immunofluorescent staining of neuronal stem cell marker SOX2 and GFAP (Leica TCS SP5 microscope). The black and white images show the positive cells for a single marker, the color image shows a composite image. **d** Percentage of marker-positive cells per arm of the protocol for cell culture GS.0875. Error bars represent differences between three different areas of the same cover slip. **e** Growth rates of the cultures from the four different arms of the protocol over three consecutive passages for three different tumors. Error bars represent the standard deviation between technical replicates.

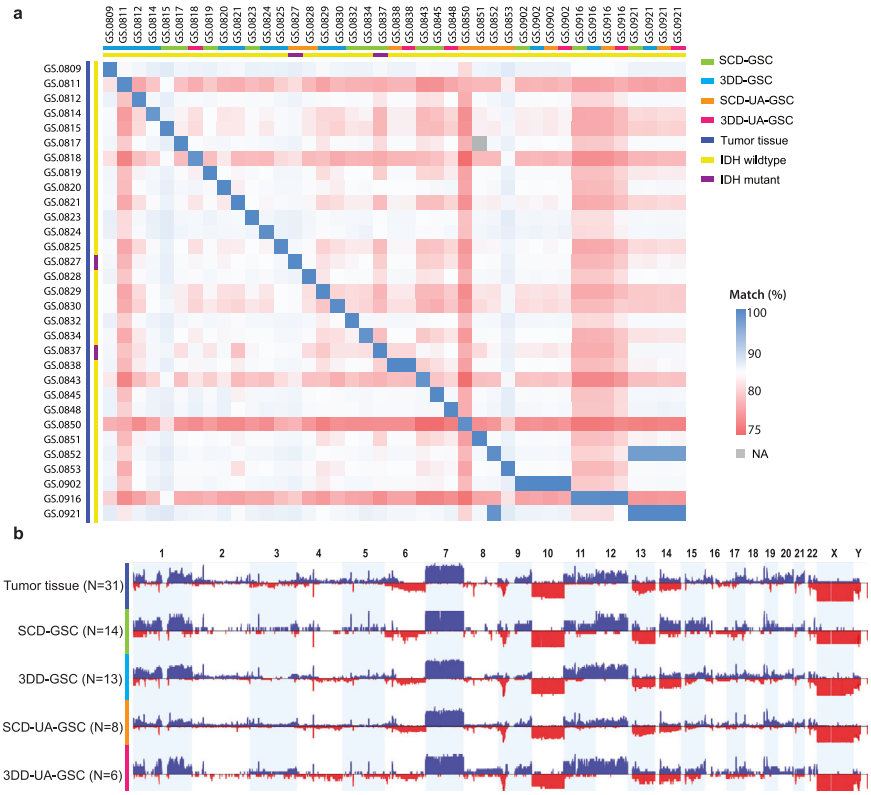

Fig. 4 | Genetic analysis of parental tissue and correspondent cell cultures. **a** Correlation matrix of sequential parental tissues and derived cell cultures. Color scale is based on the percentage match in SNPs. Blue indicates a high level of similarity, while red indicates a low level of similarity. The type of culture is denoted with colored bars, as indicated in the figure. Two sets, GS.0827 and GS.0837, were IDH1 R132H mutants, and GS.0852 and GS.0921 are a primary-recurrent set. **b** Average CNV plot for each type of glioma culture. The number of cultures used is noted on the left.

two tumors displayed different genetic profiles, and within each tumor, it was possible to observe distinct genetic subclones (Fig. 5a). The genetic heterogeneity appeared more pronounced in the earlier passages, but was independent of the resection type, suggesting that the use of different resection types allowed for establishing the tumor's genetic heterogeneity. In GS.0906 3DD-UA, we observed a subpopulation of cells characterized by fewer alterations (Astro 2), but their profile was not comparable to normal cells. Therefore, we retained them in our subsequent analysis.

To further validate the glioblastoma-specific signatures, we investigated the gene expression characteristics of genes commonly altered in HGG and of genes encoding HGG stem cell markers. These tended to be comparable between resection types and passages, indicating that despite the different resection types and passages over time, the tumors retained expression characteristics of genes with oncogenic roles in HGG (Fig. 5b). Specifically, phosphatase and tensin homolog (PTEN) expression is absent in GS.0865, aligning with SNP data indicating loss of heterozygosity (LOH) on chromosome 10. In contrast to other ex vivo HGG models, epidermal growth factor receptor (EGFR) expression was not completely lost; rather, it remained stable, which aligns with SNP data indicating chromosome 7 amplification (Fig. 5a). We also observed high and consistent expression of key stem cell markers typical of cells grown in serum-free conditions. Nevertheless, patient-specific differences in hallmark gene expression were evident, highlighting the interpatient variability characteristic of HGG.

Overall, the data indicate that our cell cultures reliably captured and maintain hallmark gene expressions specific to HGG across multiple passages, offering a valuable and consistent model for investigating treatment responses.

Single-cell RNA sequencing reveals increased heterogeneity in UA-derived cultures at early passages

To examine the transcriptomic heterogeneity within our cell cultures, we applied the shared nearest-neighbors (SNN) clustering for each patient sample over the pooled passages and resection types, and annotated the clusters based on cell types characteristic of HGG (Fig. 5c) and Neftel subtypes (Supplementary Fig. 4a–c). In a cell-culture specific analysis, UA-derived cultures exhibited greater transcriptomic heterogeneity shortly after isolation compared with resection-derived counterparts (Fig. 5d). With increasing passage number, both cell culture types revealed shifts in the composition of transcriptomic cell type populations and a general decrease in heterogeneity. Moreover, cultures from the distinct starting tissues differ in the composition of the annotated clusters. Similarly, the examination of Neftel subtypes revealed a dynamic expression pattern that varied over time and was distributed differently according to the resection type and the cell culture (Supplementary Fig. 4a, b). A more in-depth analysis indicated that not all subpopulations had significant

differences in gene expression between passages. We reported the subpopulations with significant changes in gene expression across passages in Supplementary Table 1. These results suggest that the expected variations associated with prolonged cell culturing do not occur across the entire cell population but are instead specific to a subset of cells.

Next, we addressed the effect of the resection type (traditional resection versus UA) on clustering. As shown in UMAP Fig. 5e, pooled data from all passages indicate that cells predominantly cluster based on the protocol arm through which they were derived, suggesting that distinct signatures are associated with each resection type. These signatures partially overlapped at the earliest passages (P1/P2) but diverged in

Fig. 5 | Single cell RNA sequencing shows heterogeneous cell populations within cultures. a Copy number variation (CNV) profiles of the cell cultures GS.0865 (top) and GS.0906 (bottom) subdivided by type of resection and shown across passages. The first colored bar on the left identifies the genetically diverse subclones within each condition. Each condition is depicted on the second colored bar on the left and in the legend. The red color highlights the gains, while the blue color indicates the losses in the chromosomes. **b** Dotplot showing the expression of glioblastoma hallmark genes of the cell cultures GS.0865 and GS.0906 divided by type of resection and shown across passages. **c** UMAP plot of single cells transcriptional profiling derived from cells from all tested passages and resection types from GS.0865 (top) and GS.0906 (bottom) cells. Clusters are colored and labeled by HGG-related cellular states (APC astrocyte precursor cells, OPC oligodendrocyte precursor cells, CSC cancer stem cells, Astro astrocyte-like, Oligo oligodendrocyte-like). **d** Alluvial plot showing the changes in the frequency of tumor cells clusters over time (passages) in GS.0865 3DD-GSC (top, left), GS.0865 3DD-UA-GSC (top, right), and in GS.0906 3DD-GSC (bottom, left), GS.0906 3DD-UA-GSC (bottom, right). **e** UMAP plot of GS.0865 (left) and GS.0906 (right) single cells across passages, based on the arm of the protocol through which they were derived.

Fig. 6 | Diverse sensitivity to anticancer agents in HGG cell cultures. The heatmap represents IC_{50} values, each normalized and scaled for individual drugs, spanning from 0 (minimum value and high sensitivity, yellow) to 1 (maximum value and low sensitivity, dark blue), capturing the relative range of drug concentrations tested. Light gray boxes indicate unavailable data, while dark blue boxes represent IC50 values exceeding the highest tested concentrations.

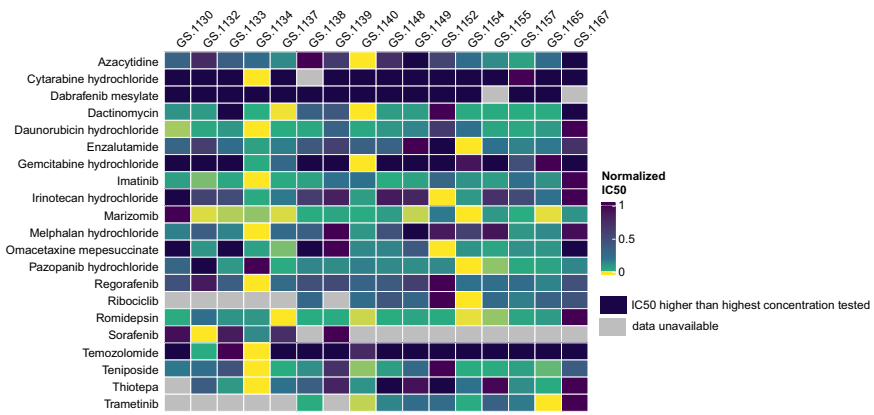

different directions during subsequent culturing. This suggests that the type of resection has a significant impact on the origin and subsequent evolution of culture composition across cultured passages. Additionally, consistent with inferred CNV results, UA-derived samples exhibit greater genetic heterogeneity at the earliest passages, as indicated by a more dispersed clustering pattern.

Gene ontology analysis of the biological processes in the earliest passages revealed that ultrasonic aspiration cultures were mainly enriched for genes related to extracellular matrix, while traditional resection samples were enriched for genes involved in nervous system development, regulation, and antigen presentation (Supplementary Fig. 4c). This may be attributed to the way ultrasonic aspiration disrupts the connection between cells and the extracellular matrix.

Taken together, resection type emerges as a significant factor influencing heterogeneity and its progression over time in cell cultures, with UA-derived samples exhibiting greater heterogeneity in the initial passages compared to traditionally resected samples.

Optimized culture protocol allows rapid personalized drug screening

To ascertain the feasibility of executing a drug screening and subsequent analysis within a clinically relevant 4-week window of tumor tissue reception, we initiated cell cultures using our refined protocol with 18 consecutive HGG samples. As a proof-of-concept, we selected 21 drugs based on potent activity in (a subset of) the high-grade glioma cultures (based on the IC_{50}), clinical relevance (e.g., previously or currently tested in clinical trials for glioblastoma patients), and/or favorable pharmacokinetic profiles for blood-brain barrier penetration as predicted by the central nervous system multi-parameter optimization (CNS-MPO) score. Moreover, we aimed to encompass a wide range of drug classes (Supplementary Table 2A). Of the 18 HGG specimens included in the study, 16 (89%) provided well-growing monolayers with sufficient cell numbers to initiate a drug screen within the set timeframe using cell cultures passages 0, 1 or 2 (Supplementary Table 2B). Analysis of the drug response curves revealed significant variations in sensitivities among the 16 screened cultures for each of the compounds (Supplementary Fig. 5, Supplementary Table 2B). The distinct drug response profiles are visualized by color-coded IC_{50} values normalized per drug, to identify the most effective compound(s) for a specific tumor (Fig. 6).

Discussion

In the past, new therapies for HGG were primarily tested on immortalized cell lines or a limited number of patient-derived cell cultures. However, given the significant inter-tumoral heterogeneity of HGG, it is crucial to have representative in vitro models encompassing all different subtypes. Furthermore, with the rise of personalized medicine in the treatment of central nervous system tumors, it becomes essential to establish reliable in vitro models for each individual patient.

For decades, serum-derived cultures were the only available option for in vitro glioma research. Over the last fifteen years, a major shift occurred towards the use of defined culture media, which selects for the propagation of GSCs. However, the success rates for adherent culture establishment remained suboptimal (~30–70%)[6,10,11,13,22]. We introduced several adjustments to our protocol, which led to a 96% overall success rate of establishing a HGG culture, which we defined as the establishment of a culture that can be passaged at least 5 times and reach a 90% confluency each time. During establishment, an estimated 5–10% of cultures drift away from the GSC genotype and phenotype. This can be assessed using CNV analysis or morphological assessment with conventional light microscopy. It is important to verify the malignant nature of the cultures in order to have a representative preclinical model.

Key factors contributing to the increased success rate include the use of 3D-derived cultures initiated from multicellular tumor fragments and the employment of ultrasound aspirate derived tumor fragments as starting material. Multicellular tumor fragments undergo less harsh treatment compared to complete dissociation into single cells, preserving their structural integrity. These fragments retain support from neighboring cells and the extracellular matrix, potentially easing their transition from the in vivo to the in vitro environment. UA-derived cultures offer a distinct advantage because the ultrasonic aspirate comprises fragments from various regions of the tumor, including areas near the tumor margins where aggressive, invading cells may be enriched. This increased heterogeneity may explain the higher success rate and faster proliferation rate compared to other arms of the protocol.

The protocol described in this work is robust and user-friendly. The samples utilized in this study were generated by multiple students and technicians in our laboratory, each independently performing the tumor processing and subsequent culturing steps after receiving appropriate training. When focusing solely on the SCD-GSC cultures, the increase in success rate in our own laboratory might be explained by the omission of serum from the collection medium in which tumor tissue was previously placed until the tissue could be processed. The differentiating capabilities of the serum may have negatively impacted the success rates in the past.

The success rate of 3DD-GSC and 3DD-UA-GSC cultures is significantly higher compared to SCD-GSC cultures. For projects where it is not crucial to culture every single tumor specimen, culturing only 3DD-(UA)-GSC may suffice for an efficient workflow. However, if the research question requires the successful establishment of a specific culture, we recommend using all four culture methods combined to maximize the chance of success.

This protocol enables early compound testing within a clinically relevant time frame in a patient-specific manner. When only a limited amount of tumor tissue is obtained from the operating theater, the number of experiments that can be performed with the tissue may be severely restricted. In such cases, rapid expansion is essential to enrich GSCs and sufficiently grow the culture to support the desired number of experiments. A growing field of research focuses on the culturing of tumor fragment-derived tumoroids or organotypic spheroids from glioma tissue samples[12,23–25]. While acknowledging the utility and increased complexity of these model systems, it is important to note that their potential for expansion in the same composition is limited, as most supporting cells are post-mitotic. Additionally, the 3D structures are less compatible with fully automated procedures, such as automated pipetting systems, and require more laborious techniques for drug response assessment compared to 2D cultures. The culture methods presented in this work have limitations similar to those of other two-dimensional culture protocols, such as differences in the microenvironment compared to the in-situ situation, lack of interaction with glial cells, lack of interaction with the immune system, and absence of a blood-brain barrier. When the answer to a research question depends on these variables, an appropriate model should be chosen.

The culture method presented in this study supports the long-term expansion of HGG glioma cultures, enabling the establishment of a biobank that serves as an invaluable resource for target identification, drug development, and repurposing studies. The availability of genetically diverse cultures is essential for large-scale experiments and is of significant benefit to the scientific community. The high success rate of this culture protocol greatly facilitates the inclusion of the near-complete spectrum of subtypes of HGG into the biobank. Moreover, we recently reported that monolayer drug screening on patient-derived cultures with passage numbers ranging from 6–10 predicted patient response to temozolomide (TMZ) more specifically than methylguanine methyltransferase (MGMT) promoter methylation status[14]. The study also identified 21 genes related to TMZ sensitivity, which could be validated in external data sets. This highlights the valuable role that biobanks of GSC cultures can play in preclinical and clinical research.

Single-cell sequencing indicated that 3DD-UA-derived cultures exhibit more heterogeneity in the first passages after isolation compared to 3DD-GSC cultures. The increased (peri)tumoral area probed and sampled through ultrasonic aspiration results in the collection of tissue with greater diversity, potentially facilitating the expansion of invasive cell subpopulations not present in samples derived solely from a resection sample. Moreover, upon subsequent culturing and passaging, the transcriptomic signatures evolved in different directions between UA and sample-derived cultures. The different initial composition can explain the subsequent divergence during culturing and could influence the adaptability to in vitro cell culture conditions. Alternatively, the process of UA may leave an imprint on the single-cell gene expression profile, influencing subsequent passages. Nevertheless, all culture types retained profiles characteristic of HGG up to at least passage 11. Transcriptomics data did show shifts in the composition of transcriptomic cell subpopulations and a decrease in heterogeneity with increasing passage number. Therefore, we recommend utilizing the lowest passage possible, ideally below passage 5, for (pre-) clinical testing.

A proof-of-concept study was performed to assess the feasibility of conducting and analyzing a 20-drug screen on patient-derived HGG cells, while taking into account the typical timeframe between surgery and treatment initiation, which averages approximately 4 weeks. Notably, we successfully conducted the drug screen within this critical window for 16 out of 18 (89%) consecutive HGG samples. The outcomes of these screens underscored the substantial heterogeneity in drug sensitivities among the different HGGs, emphasizing the need for precision therapy. By applying the different arms of the protocol in parallel, we managed to establish a successful culture within 3 weeks for the majority of patients, offering the prospect of implementation of our platform for future guiding of therapy selection. It is important to note, however, that also for patient-tailored therapies, the identification of more efficacious compounds for HGG is urgently needed. Current advancements focused on the development of targeted molecular therapies[26,27], as well as the increased efforts in assessing the efficiency of therapeutic agents to reach the target sites within the brain[28,29] are anticipated to contribute to the identification of more effective therapeutics for patients with HGGs.

Taken together, our culture protocol has demonstrated its high efficiency in establishing cell cultures from the majority of HGG samples in a reproducible and timely manner. This not only facilitates the exploration of potential new therapies for HGG but also represents a significant step in the development of patient-specific medicine approaches for this patient group.

Methods

Tumor processing and cell culture establishment

This study adhered to the ethical standards set by the Institutional Review Board of Erasmus MC and the Declaration of Helsinki. Prior to the collection of human material, informed consent was obtained from all participants (or their legal guardians). The Institutional Review Board approved all procedures involving tissue samples under protocol number MEC-2013-090 (6 February 2013). Samples included in this study are graded according to the World Health Organization (WHO) 2016 classification as either 'glioblastoma, IDH wildtype', or 'glioblastoma, IDH mutant', with a histopathological grade of WHO grade IV[30]. These samples are collectively referred to as HGG samples in this manuscript. The samples were processed using an optimized protocol based on our previous studies[6,21]. Ultrasonic aspirated tissue fragments were collected in a tissue trap fitted into the collection system of a Cavitron ultrasonic aspirator[31]. This prevents prolonged exposure of the tissue fragments to the saline-erythrocyte mixture in the container. Resected tissue and UA tissue fragments were collected in DMEM (Gibco) without additives and stored at 4 °C until processing, typically within 6 h. The samples were mechanically dissociated using a scalpel until the resulting pieces were approximately 0.5–2 mm in size and fit through a 10 ml pipette. The samples were then washed and subjected to enzymatic dissociation using Collagenase A (Roche) and DNAse (Roche). Subsequently, the suspension was strained through a 70 µm filter to separate single cells from larger fragments. The single cells (SCD) in the sifted material and larger fragments (3DD) that remain on top of the filter were then transferred to separate uncoated culture flasks for initial non-adherent culture.

In some cases, only small biopsies (SB) were available. For these samples, we omitted the enzymatic dissociation and filtration steps and directly transferred finely chopped tumor pieces into a small non-coated culture flask with culture medium (SB-GSC culture).

Cell culture

After 5–8 days, the cultures were transferred to a new flask coated with 1:100 diluted PathClear Cultrex Reduced Growth Factor Basement Membrane Extract (BME, R&D Systems). Any adherent cells were detached with a scraper, and the cell suspension was transferred along with the suspended cells. Before coating, the flasks were briefly washed with phosphate-buffered

saline (PBS) to remove any electrostatic tension. Aliquoted BME was diluted 1:10 in cold culture medium and added to the culture flasks (300 µl for T25, 500 µl for T75, 1 ml for T175), spread out evenly by tilting the flask, and incubated at 37 °C for at least 30 min prior to use, or for up to 10 days for later use. Cell suspensions were added to the flasks without the need for extra washing steps. Cultures were inspected every three to four days and passaged when the flasks were more than 90% confluent or if there were multiple areas in the flasks with very high cell density. For passaging, cells were detached with Accutase (Gibco) by incubation for 5–10 min, washed with PBS, centrifuged in a 15 ml centrifuge tube at 1500 rotations per minute for 3 min, and resuspended in fresh medium, typically at a ratio of 1:3–1:6, depending on growth rate. Cultures were defined as "successful" if they could be passaged at least five times and reach 90% confluency each time.

Bright field microscopy

Bright field microscopy images were made on a routine basis with a Zeiss Axio Observer D1 Inverted Phase Contrast Fluorescence Microscope, HAL1 illuminator, and using a 10x Zeiss A-plan objective (421041-9910-000).

Growth rate analysis

Cells were counted using the Countess automated cell counter and seeded in triplicate into BME-coated T25 flasks at a density of 100,000 cells per flask. After 4–6 days, the medium was removed, cells were detached with Accutase (Gibco), and the cell count was determined using the Countess. The exponential growth rate for each sample was then calculated. Standard deviation was assessed based on the variation between the three technical replicates. Multifactorial linear regression was performed using R, with P-values adjusted via Bonferroni correction for 10 factors in the regression model.

Immunofluorescent staining

Cells were seeded on coverslips coated with a 1:20 dilution of PathClear Cultrex Reduced Growth Factor BME (R&D Systems) in 6-well plates at a density of 75,000 cells per well. The plates were incubated at 37 °C for 24 h, then fixed with 2% paraformaldehyde (PFA) and washed with PBS. Coverslips were stored in PBS at 4 °C until staining. Primary antibodies were diluted and applied to the cells (mouse-anti-GFAP, IF03l, Millipore,1:200 dilution, and goat-anti-SOX2, GT15098, Immune Systems, 1:200 dilution), followed by overnight incubation at 4 °C. The next day, the coverslips were incubated with secondary antibodies for 1 h at room temperature (Donkey-anti-Goat IgG, DyLight 488, NBP1-74817, Novus Biologicals, 1:500 dilution and donkey-anti-mouse IgG, AF647, Ab150107, Abcam, 1:1000 dilution). Coverslips were mounted using VectaShield with DAPI (Vector Laboratories, H-1200-10) and sealed with clear nail polish. Images were captured using a Leica TCS SP5 microscope and LAS X software, with images taken from three different areas of each slide. Images were stacked and analyzed in ImageJ, and the percentage of marker-positive cells relative to the total number of DAPI+ nuclei was recorded.

Nucleic acid extraction

Cultured cells were collected during regular passaging. Cell pellets were snap frozen, and Genomic DNA was extracted from snap frozen cell pellets and from cryosections of liquid N_2 stored snap frozen tumor material. All DNA was isolated with the DNeasy Blood & Tissue Kit (Qiagen) according to the manufacturer's instructions. The Qubit dsDNA HS assay was used to determine DNA concentrations.

Global screening array

To assess CNV profiles of 31 patient tissues and their derived cell cultures, 200 ng of DNA from each sample was loaded according to the manufacturer's instructions on an Illumina Infinium Global Screening Array (Illumina, 20024620) v2.0 chip, which probes ~760k SNPs. GenomeStudio software (Illumina) was used to analyze CNV GSA manifest files. Final reports and visualizations were created using the Nexus Discovery software package (BioDiscovery, El Segundo). The minimum number of probes per segment was set to 20, and the minimum LOH length to 500 kB.

Single-cell RNA sequencing

Single-cell RNA sequencing was performed on a 3DD-GSC culture and a 3D-UA-GSC culture derived from two primary HGG patients: GS.0865 and GS.0906. For each patient, cells were collected from each culture type for analysis at passages P1/P2, P5, P11, and P16. Cell cultures were washed with PBS and incubated with Accutase (Gibco) for 10–15 min, and collected in Hank's balanced salt solution (HBSS). Cells were centrifuged and resuspended in HBSS (Gibco), and subsequently sorted with FACSAria II (BD Biosciences) into 384-well plates based on single-cell selection gating. Cells were then subjected to single-cell transcriptomic sequencing (SORT-seq) as previously described[32]. Briefly, single cells sorted into 384-well plates were submitted for single-cell cell RNA sequencing at Single Cell Discoveries, Utrecht. Libraries were constructed based on a semi-robotized implementation of the CELseq2 library protocol and submitted for paired-end sequencing. The sequencing was performed with Illumina NextSeq 500[32]. In total, 3840 cells (GS.0865 $n = 2304$; GS.0906 n = 1536) were sequenced.

Single-cell RNA sequencing analysis

Analysis of the scRNAseq data was performed in R using the Seurat package (v3.2.0)[33]. Briefly, per patient, the low-quality cells were filtered (GS.0865 $n = 760$; GS.0906 $n = 291$), followed by data normalization as implemented in Seurat[34]. As the cell clustering is based on the cell cycle phase, this heterogeneity was regressed out. Finally, the cells were clustered using Seurat's FindNeighbors and FindClusters functions, with a resolution of 0.5. The results were visualized with uniform manifold approximation and projection (UMAP) plots. Each cluster was annotated using the scCATCH package, employing "Glioma" and "Glioblastoma" as the reference type of human cancer tissue[35]. To identify the GBM cellular states derived from Neftel et al.[4], Seurat's function AddModuleScore was used. The highest module score for each cell defined the cellular state.

All comparisons aimed to identify differentially expressed genes, which were determined by applying the FindAllMarkers function with a non-parametric Wilcoxon rank-sum test (Bonferroni-adjusted p-value < 0.05). The differentially expressed genes derived from the differences between UA and traditional resection at passage 1 (p01), with a threshold of log2FC > 1, were used to perform gene enrichment analysis for gene ontology (GO) and biological processes. The GO analysis was conducted using the enrichGO function from the clusterProfiler package[36].

Copy number variation was inferred using the inferCNV package, with astrocytes from the GSE171684 study serving as normal cells[37]. The analysis mode was based on samples.

Drug screening

For the drug screening studies, we tested a total of 21 U.S. Food and Drug Administration (FDA) approved oncology drugs. Compounds were selected from the FDA-approved Oncology Drug Set II library (National Cancer Institute) based on several factors, including cell killing efficacy on primary glioma cultures at clinically feasible concentrations, the inclusion of compounds from several different drug classes, and the pharmacokinetic profiles based on the central nervous system multi-parameter optimization (CNS-MPO) score. For a detailed description of the methodology, please see our earlier work by Ntafoulis et al.[38]. The compounds Azacytidine (SelleckChem), Cytarabine hydrochloride (Sigma-Aldrich), Dabrafenib mesylate (Toronto Research Chemicals), Dactinomycin (BioViotica), Daunorubicin hydrochloride (SelleckChem), Enzalutamide (MedChem Express), Gemcitabine hydrochloride (Sigma-Aldrich), Imatinib (SelleckChem), Irinotecan hydrochloride (Cayman Chemical Company), Marizomib (Sigma-Aldrich), Melphalan hydrochloride (Sigma-Aldrich), Omacetaxine mepesuccinate (Sigma-Aldrich), Pazopanib hydrochloride (Sigma-Aldrich), Regorafenib (MedChem Express), Ribociclib (MedChem Express), Romidepsin (MedChem Express), Sorafenib (Sigma-

Aldrich), Temozolomide (Sigma-Aldrich), Teniposide (Santa Cruz Biotechnology, Inc.), Thiotepa (Sigma-Aldrich), and Trametinib (MedChem Express) were selected for the proof-of-concept screenings. Screens were performed as described previously[21]. Briefly, using an automated pipetting system (Hamilton), GSCs were seeded at a density of 500 cells/well in quadruplicates in 384-well plates pre-coated with 10 µl/well of 1:100 diluted Cultrex Reduced Growth Factor BME (R&D Systems). After 24 h, 8–10 step serial dilutions of 21 drugs and dimethylsulfoxide (DMSO) solvent were prepared in culture medium and added to the wells, with a final total volume of 85 µl/well. The concentration of DMSO was dependent on the concentration of the compounds, with a maximum of 1%. A control dilution series of DMSO was added to correct for any DMSO effects on viability. After five days of exposure, cell viability was measured with the ATP-based CellTiter Glo 2.0 kit (Promega), and luminescence was measured using the Infinite 200 reader (Tecan). The IC50 values were calculated from the averaged values by applying a nonlinear regression (curve-fit) analysis and selecting the dose versus normalized response inhibition equation in GraphPad Prism.

Statistical analysis

Fisher's exact test (two-sided) was applied to determine if the efficiency of established cell cultures obtained from single cells of resected tissue (SCD-GSC) was statistically different from those derived from large fragments (3DD-GSC), as well as cultures obtained through ultrasonic aspiration (SCD-UA-GSC and 3DD-UA-GSC), and cell cultures derived from small biopsies (3DD-SB-GSC).

Paired t-test (two-tailed) was applied to determine the difference of tumor quantity between samples of the same tumor derived from traditional resection and ultrasonic aspirates. Results are reported as mean ± standard deviation (SD).

In all tests, a p value < 0.05 was adopted to establish statistical significance. The analyses were performed in GraphPad Prism.

Data availability

The datasets generated and/or analyzed during the current study are available in the Gene Expression Omnibus Repository, Accession number: GSE248544.

Code availability

All relevant R scripts are available from the corresponding authors upon reasonable request. Detailed information regarding the software used for the different analyses can be found in the Methods section.

Received: 25 November 2023; Accepted: 8 May 2025;
Published online: 27 May 2025

References

1. Ostrom, Q. T. et al. CBTRUS Statistical Report: Primary brain and other central nervous system tumors diagnosed in the United States in 2015–2019. *Neuro-Oncol.* **24**, v1–v95 (2022).
2. Patel, A. P. et al. Single-cell RNA-seq highlights intratumoral heterogeneity in primary glioblastoma. *Science* **344**, 1396–1401 (2014).
3. Pesenti, C. et al. The genetic landscape of human Glioblastoma and matched primary cancer stem cells reveals intratumour similarity and intertumour heterogeneity. *Stem Cells Int.* **2019**, 1–12 (2019).
4. Neftel, C. et al. An Integrative model of cellular states, plasticity, and genetics for Glioblastoma. *Cell* **178**, 835–849.e821 (2019).
5. Lee, J. et al. Tumor stem cells derived from glioblastomas cultured in bFGF and EGF more closely mirror the phenotype and genotype of primary tumors than do serum-cultured cell lines. *Cancer Cell.* **9**, 391–403 (2006).
6. Balvers, R. K. et al. Serum-free culture success of glial tumors is related to specific molecular profiles and expression of extracellular matrix–associated gene modules. *Neuro-Oncol.* **15**, 1684–1695 (2013).
7. Singh, S. K. et al. Identification of human brain tumour initiating cells. *Nature* **432**, 396–401 (2004).
8. Günther, H. S. et al. Glioblastoma-derived stem cell-enriched cultures form distinct subgroups according to molecular and phenotypic criteria. *Oncogene* **27**, 2897–2909 (2008).
9. Laks, D. R. et al. Neurosphere Formation Is an Independent Predictor of Clinical Outcome in Malignant Glioma. *Stem Cells* **27**, 980–987 (2009).
10. Xie, Y. et al. The human Glioblastoma cell culture resource: validated cell models representing all molecular subtypes. *EBioMedicine* **2**, 1351–1363 (2015).
11. Grube S., Freitag D., Kalff R., Ewald C., Walter J. Characterization of adherent primary cell lines from fresh human glioblastoma tissue, defining glial fibrillary acidic protein as a reliable marker in establishment of glioblastoma cell culture. *Cancer Rep*. **4**, e1324 (2021).
12. Jacob, F. et al. A patient-derived Glioblastoma organoid model and biobank recapitulates inter- and intra-tumoral heterogeneity. *Cell* **180**, 188–204.e122 (2020).
13. Mullins, C. S. et al. Establishment and characterization of primary glioblastoma cell lines from fresh and frozen material: a detailed comparison. *PLoS One* **8**, e71070 (2013).
14. Ntafoulis, I. et al. Ex vivo drug sensitivity screening predicts response to temozolomide in glioblastoma patients and identifies candidate biomarkers. *Br. J. Cancer* **129**, 1327–1338 (2023).
15. Howard, C. M. et al. Analysis of chemopredictive assay for targeting cancer stem cells in Glioblastoma patients. *Transl. Oncol.* **10**, 241–254 (2017).
16. Stockslager, M. A. et al. Functional drug susceptibility testing using single-cell mass predicts treatment outcome in patient-derived cancer neurosphere models. *Cell Rep.* **37**, 109788 (2021).
17. Henzi, S., Krayenbühl, N., Bozinov, O., Regli, L. & Stienen, M. N. Ultrasonic aspiration in neurosurgery: comparative analysis of complications and outcome for three commonly used models. *Acta Neurochirurg.* **161**, 2073–2082 (2019).
18. Jallo G. I. CUSA EXcel Ultrasonic Aspiration System. **48**, 695–697 (2001).
19. Beckner, M. E. et al. Tumor cells from ultrasonic aspirations of glioblastomas migrate and form spheres with radial outgrowth. *Cancer Lett.* **255**, 135–144 (2007).
20. Day, B. et al. Glioma surgical aspirate: a viable source of tumor tissue for experimental research. *Cancers* **5**, 357–371 (2013).
21. Verheul, C. et al. Generation, characterization, and drug sensitivities of 12 patient-derived IDH1-mutant glioma cell cultures. *Neuro-Oncol. Adv.* **3**, vdab103 (2021).
22. Pollard, S. M. et al. Glioma stem cell lines expanded in adherent culture have tumor-specific phenotypes and are suitable for chemical and genetic screens. *Cell. Stem Cell.* **4**, 568–580 (2009).
23. Hubert, C. G. et al. A three-dimensional organoid culture system derived from human glioblastomas recapitulates the hypoxic gradients and cancer stem cell heterogeneity of tumors found in vivo. *Cancer Res.* **76**, 2465–2477 (2016).
24. De Witt Hamer, P. C. et al. The genomic profile of human malignant glioma is altered early in primary cell culture and preserved in spheroids. *Oncogene* **27**, 2091–2096 (2008).
25. Golebiewska, A. et al. Patient-derived organoids and orthotopic xenografts of primary and recurrent gliomas represent relevant patient avatars for precision oncology. *Acta Neuropathol.* **140**, 919–949 (2020).
26. El Atat, O., Naser, R., Abdelkhalek, M., Habib, R. A. & El Sibai, M. Molecular targeted therapy: A new avenue in glioblastoma treatment (Review). *Oncol. Lett.* **25**, 46 (2023).
27. Yang, K. et al. Glioma targeted therapy: insight into future of molecular approaches. *Mol. Cancer* **21**, 39 (2022).

28. Vogelbaum, M. A. et al. A window of opportunity to overcome therapeutic failure in neuro-oncology. *Am. Soc. Clin. Oncol. Educ. Book.* **42**, 1–8 (2022).
29. Cho, N. S., Wong, W. K., Nghiemphu, P. L., Cloughesy, T. F. & Ellingson, B. M. The future Glioblastoma clinical trials landscape: Early Phase 0, window of opportunity, and adaptive Phase I-III studies. *Curr. Oncol. Rep.* **25**, 1047–1055 (2023).
30. Louis, D. N. et al. The 2016 World Health Organization Classification of Tumors of the Central Nervous System: a summary. *Acta Neuropathol.* **131**, 803–820 (2016).
31. Martirosian, V. et al. Utilization of discarded surgical tissue from ultrasonic aspirators to establish patient-derived metastatic brain tumor cells: a guide from the operating room to the research laboratory. *Curr. Protoc.* **1**, e140 (2021).
32. Muraro, M. et al. A single-cell transcriptome atlas of the human pancreas. *Cell Syst.* **3**, 385–394.e383 (2016).
33. Butler, A., Hoffman, P., Smibert, P., Papalexi, E. & Satija, R. Integrating single-cell transcriptomic data across different conditions, technologies, and species. *Nat. Biotechnol.* **36**, 411–420 (2018).
34. Ilicic, T. et al. Classification of low quality cells from single-cell RNA-seq data. *Genome Biol*. **17**, 29 (2016).
35. Shao, X. et al. scCATCH: Automatic annotation on cell types of clusters from single-cell RNA sequencing data. *iScience* **23**, 100882 (2020).
36. Yu, G., Wang, L.-G., Han, Y. & He, Q.-Y. clusterProfiler: an R package for comparing biological themes among gene clusters. *OMICS: J. Integr. Biol.* **16**, 284–287 (2012).
37. Kihara Y. et al. Ponesimod inhibits astrocyte-mediated neuroinflammation and protects against cingulum demyelination via S1P 1 -selective modulation. *FASEB J*. **36**, e22132 (2022).
38. Ntafoulis, I. et al. A repurposed drug selection pipeline to identify CNS-penetrant drug candidates for Glioblastoma. *Pharmaceuticals* **17**, 1687 (2024).

Acknowledgements

We thank all patients for contributing to this research and the neurosurgeons involved for providing the tissue. We also acknowledge Stichting STOPHersentumoren, Erasmus Foundation-Brain Tumor Survival Marathon, and Erasmus Foundation-Stichting de Merel for funding this research.

Author contributions

Conceptualization: C.P.V., M.L.M.L., S.L. Experimental design: C.P.V., M.L.M.L. Acquisition and processing of tumor samples: C.P.V., C.D.H., R.B., T.V.K., J.V.D.B. Acquisition of DNA sequencing data: B.E., A.D.K. Acquisition of RNA data: K.J.F., M.P.C. Immunocytochemistry: J.H. Drug screening: C.D.H., I.N. Analysis and interpretation of data: C.P.V., F.F., I.V., K.J.F., M.P.C., S.L., M.L.M.L. Funding acquisition/Project administration: M.L.M.L., C.M.F.D. Supervision: S.L., M.L.M.L. Writing-original draft: C.P.V., F.F., M.L.M.L. Writing-review & editing: C.P.V., F.F., I.V., R.B., B.E., A.D.K., C.M.F.D., S.L., M.L.M.L.

Competing interests

The authors declare no competing interests.

Additional information

Supplementary information The online version contains supplementary material available at https://doi.org/10.1038/s41698-025-00946-1.

Correspondence and requests for materials should be addressed to Martine L. M. Lamfers.